Colloid & Polymer Sci. **255**, 460–467 (1977)

ISSN 0303-402X / ASTM-Coden: CPMSB (formerly KZZPAF)

Pulp and Paper Research Institute of Canada and Department of Chemistry, McGill University, Montreal (Canada)

A rigorous theory of ring tensiometry: addendum on the wall effect

C. Huh and *S. G. Mason*

With 4 figures and 1 table

(Received January 12, 1976)

Nomenclature

a	=	radius of cylinder or ring wire; $\bar{a} \equiv a\sqrt{C_{23}}$
C_{23}	=	$(\varrho_2 - \varrho_3)\, g/\gamma_{23}$
D	=	semi-gap width between parallel walls, or radius of liquid container; $\bar{D} \equiv D\sqrt{C_{23}}$
f	=	*Harkins-Jordan* (1) factor
F, E	=	elliptic integrals of the first and second kind (k = modulus)
F	=	equilibrium capillary force on ring or per unit length of a straight cylinder; $\bar{F} = F\sqrt{C_{23}}/\gamma_{23}$
F_D, F_∞	=	maximum F for finite D and $D = \infty$
g	=	gravity
r_i, z_i	=	r- and z-coordinates of the inner ($i = 1$) and outer ($i = 2$) contact line circles on ring; $\bar{r}_i \equiv r_i\sqrt{C_{23}}$, $\bar{z}_i \equiv z_i\sqrt{C_{23}}$
z_c	=	vertical coordinate of the contact line on cylinder; $\bar{z}_c \equiv z_c\sqrt{C_{23}}$
γ_{23}, γ_D	=	interfacial tension ($D = \infty$); uncorrected interfacial tension measured in container of radius D
ϱ_i	=	density of the i phase
ϕ_i	=	slope angle of the inner ($i = 1$) and outer ($i = 2$) menisci on ring
$180° - \phi_c$	=	slope angle of cylindrical meniscus at the contact line
ψ_2	=	$180° - \phi_2$
θ_0	=	contact angle at container wall
Δ	=	$(F_D - F_\infty)/F_\infty$ for cylinder; $(\gamma_D - \gamma_{23})/\gamma_{23}$ for ring

I. Introduction

The success of the ring method (1, 2) for measuring surface and interfacial tensions of liquids by pulling a ring through an interface rests, among many factors, on the flatness of the liquid interface at large distance from the ring center. This requires employing large amounts of test liquids to provide an interface large enough so that there is no wall effect. Since issuing our paper on the theory of ring tensiometry (2),*) questions have been raised about correcting for wall effects and how large the container must be before the corrections become negligible. In this addendum we examine the effect of the wall on the measurement.

Since precise theoretical calculations of the wall effect are difficult because of the inordinate amount of numerical computations required, we aim here to determine the parameters which can cause the errors and to estimate their magnitude. It is seen that unless the density difference across the interface is very small or the interfacial tension is very large, the wall effect is generally small and can easily be rendered negligible.

As a preliminary step, we first study the simpler problem of pulling an infinitely-long, horizontal circular cylinder of radius a through a liquid interface confined between two vertical plates separated by $2D$ (fig. 1 insets). The maximum pull F_∞ on the cylinder per unit length through an infinitely-large interface has been studied by *Princen* and *Mason* (3), and we compare their results with the maximum pull F_D through a finite interface.

The maximum force F_D on the circular ring pulled through a liquid interface which is confined in a container of finite radius D, is then approximately calculated and compared with the force F_∞ for the infinitely large interface. The force F_D depends not only on

*) The new address for ordering the 97-page numerical tabulation of ref. (2) (NAPS document No. 02823) is ASIS/NAPS % Microfiche Publications, P.O. Box 3513, Grand Central Station, New York, N.Y. 10017.

D but also on the condition of the interface at the container wall and on the initial shape of interface. If the interface makes a constant contact angle θ_0 (measured through the lower phase) with the container wall, F_D varies with θ_0; if the contact line of the interface is attached to the edge of the container rim and remains there, F_D depends on whether the interface is initially convex or concave (viewed downwards from the top). In the following theoretical derivations, we assume that the liquid interface makes a constant contact angle θ_0 with the vertical of the container, with no contact angle hysteresis.

In section IV we report experimental measurements of the surface tension of water in air measured in different size containers.

As before (2), we use the following dimensionless variables:

$$\bar{a} \equiv a\sqrt{C_{23}};\ \bar{R} \equiv R\sqrt{C_{23}};\ \bar{D} \equiv D\sqrt{C_{23}};$$
$$\bar{F} \equiv F\sqrt{C_{23}}/\gamma_{23}$$

where $C_{23} \equiv (\varrho_2 - \varrho_3)\, g/\gamma_{23}$; ϱ_3 and ϱ_2 are the respective densities of the upper and lower phases; g is gravity; γ_{23} is the interfacial tension; R is the ring radius; and a the wire (or cylinder) radius. We arbitrarily set $F \equiv 0$ when the cylinder or the ring is completely in the lower phase.

II. Horizontal circular cylinder

When an infinitely-long, horizontal circular cylinder is pulled under equilibrium conditions through a liquid interface, the force per unit length on the thread attached to it in dimensionless quantities is:

$$\bar{F} = \sin\phi_c + \int_{\phi_c}^{\pi} [-\bar{z}_c + \bar{a}(\cos\phi_c - \cos\phi)]\, \bar{a}\cos\phi\, d\phi$$
$$= \sin\phi_c + \bar{z}_c\bar{a}\sin\phi_c - \frac{\bar{a}^2}{2}\left(\frac{1}{2}\sin 2\phi_c + \pi - \phi_c\right) \qquad [1]$$

where $(180° - \phi_c)$ is the slope angle of the meniscus at the contact line, and $z_c \equiv \bar{z}_c/\sqrt{C_{23}}$ is the contact line height. We assume that the contact angle is zero on the ring or cylinder surface. The meniscus shape formed around the cylinder depends on the condition observed at the container wall; we will study the cases where $\theta_0 = 0°$, 90° and 180° at the wall.

At the maximum $\bar{F}_D$:

$$\frac{d\bar{F}}{d\phi_c} = 0 = \cos\phi_c + \bar{a}\left(\frac{d\bar{z}_c}{d\phi_c}\sin\phi_c + \bar{z}_c\cos\phi_c\right) + \bar{a}^2\sin^2\phi_c\,. \qquad [2]$$

(i) *When $\theta_0 = 0°$ at the wall*

The meniscus formed is concave when viewed from the top, and we obtain from its shape ([32–33] - 4*)

$$\bar{z}_c = 2\left[\frac{1}{k^2} - \cos^2\left(\frac{\phi_c}{2}\right)\right]^{\frac{1}{2}}, \qquad [3]$$

$$\bar{D} - \bar{a}\sin\phi_c = \left(\frac{2}{k} - k\right)\left[2F\left(k, \frac{\pi}{2}\right) - F\left(k, \frac{\pi - \phi_c}{2}\right) - F\left(k, \frac{\pi}{4}\right)\right] - \frac{2}{k}\left[2E\left(k, \frac{\pi}{2}\right) - E\left(k, \frac{\pi - \phi_c}{2}\right) - E\left(k, \frac{\pi}{4}\right)\right] \qquad [4]$$

where F and E are elliptic integrals of the first and second kind, respectively.

Differentiating [3] and [4], we get

$$\frac{d\bar{z}_c}{d\phi_c} = \left(\sin\phi_c - \frac{4}{k^3}\frac{dk}{d\phi_c}\right)/\bar{z}_c\,, \qquad [5]$$

$$\cos\phi_c\left(\bar{a} + \frac{k}{2\sqrt{1 - k^2\cos^2\left(\frac{\phi_c}{2}\right)}}\right) = \frac{dk}{d\phi_c}\left[\frac{(1 - 2/k^2)}{(1 - k^2)}\left\{2E\left(k, \frac{\pi}{2}\right) - E\left(k, \frac{\pi - \phi_c}{2}\right) - E\left(k, \frac{\pi}{4}\right)\right\} + \frac{2}{k^2}\left\{F\left(k, \frac{\pi}{2}\right) - F\left(k, \frac{\pi - \phi_c}{2}\right)\right.\right.$$

*) designating Eqs. [32] and [33] of ref. (4).

$$- F\left(k, \frac{\pi}{4}\right)\Bigg\} + \frac{(k^2/2-1)}{(1-k^2)} \times \left\{ \frac{\sin\left(\frac{\phi_c}{2}\right)}{\sqrt{1-k^2\cos^2\left(\frac{\phi_c}{2}\right)}} + \frac{1}{\sqrt{1-k^2/2}} \right\} \Bigg] . \qquad [6]$$

Inserting [3], [5] and [6] into [2], we first eliminate $\bar{z}_c$ and $d\bar{z}_c/d\phi_c$ from [2]; we then calculate k and ϕ_c from [2] and [4] for given $\bar{D}$ and $\bar{a}$. This calculation in reality requires a successive approximation method, and has been done on an IBM S360 computer employing a standard subroutine for obtaining roots of non-linear equations. Once ϕ_c and k are known, we can calculate $\bar{F}_D$ from [1], and compare it with $\bar{F}_\infty$ for $\bar{D} \to \infty$ (thus $k = 1$). Fig. 1 (a) shows the results of calculations, $\Delta \equiv (F_D - F_\infty)/F_\infty$ in percentage as a function of D/a and $\bar{a}$.

(ii) *When $\theta_0 = 180°$ at the wall*

When the upper phase wets the container wall, the meniscus has an inflexion point (4) and is different from the above (see inset of fig. 1 (b)); we get instead of [3] and [4]

$$\bar{z}_c = 2\left[k^2 - \cos^2\left(\frac{\phi_c}{2}\right)\right]^{\frac{1}{2}}, \qquad [7]$$

$$\bar{D} - \bar{a}\sin\phi_c = 2E(k, \psi_c) + 2E(k, \psi_w) - F(k, \psi_c) - F(k, \psi_w) - 4E\left(k, \frac{\pi}{2}\right) + 2F\left(k, \frac{\pi}{2}\right), \qquad [8]$$

where

$$\psi_c \equiv \sin^{-1}\left(\frac{1}{k}\cos\frac{\phi_c}{2}\right) \text{ and } \psi_w \equiv \sin^{-1}(1/\sqrt{2}k).$$

We can again calculate k and ϕ_c from [2] and [8] at the maximum pull for given $\bar{a}$ and $\bar{D}$; and then $\bar{F}_D$ from [1]. Fig. 1 (b) shows Δ in percentage as a function of D/a and $\bar{a}$.

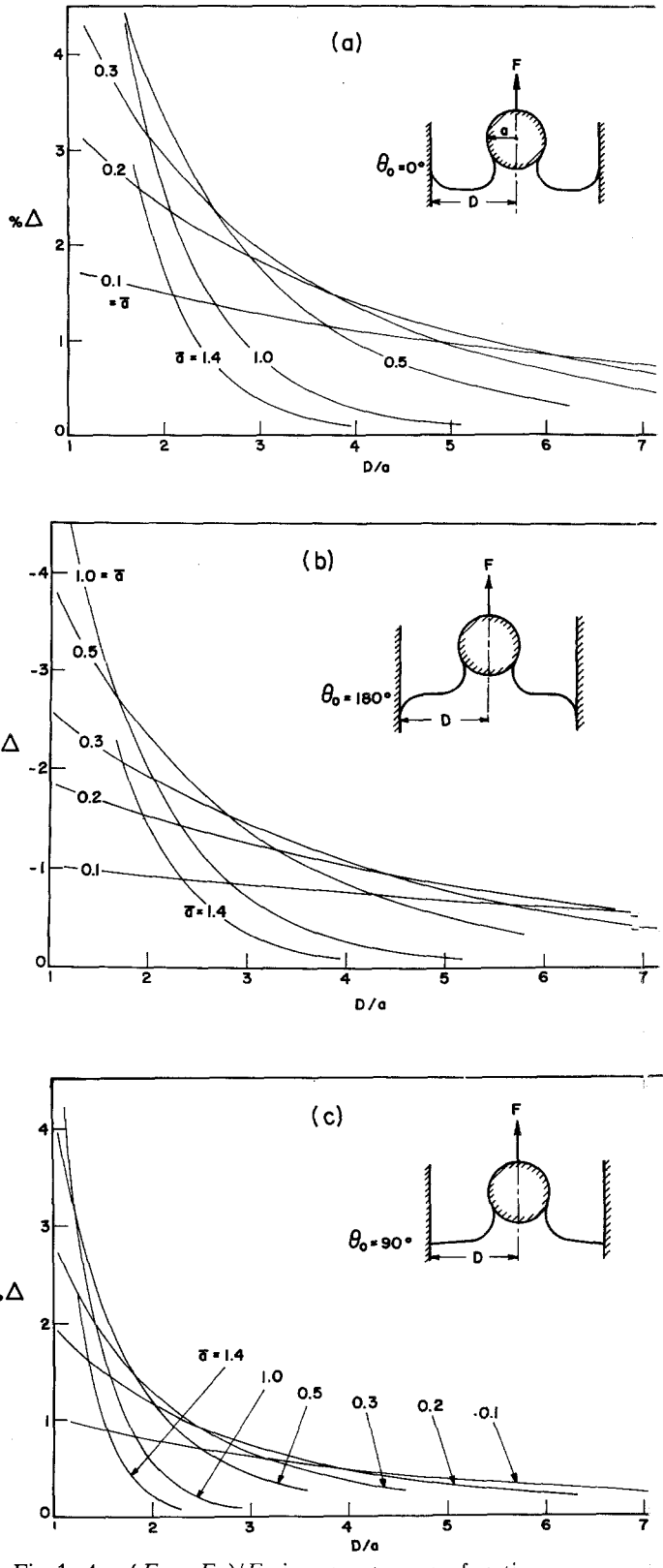

Fig. 1. $\Delta \equiv (F_D - F_\infty)/F_\infty$ in percentage as a function of D/a and $\bar{a}$. (a) $\theta_0 = 0°$; (b) $\theta_0 = 180°$; and (c) $\theta_0 = 90°$ at container wall

(iii) *When $\theta_0 = 90°$ at the wall*

Here [1] to [3] apply and only [4] differs:

$$\bar{D} - \bar{a}\sin\phi_c = \acute{k}\left[\left(\frac{2}{k^2} - 1\right)\left\{F\left(k, \frac{\pi}{2}\right) - F\left(k, \frac{\pi - \phi_c}{2}\right)\right\} - \frac{2}{k^2}\left\{E\left(k, \frac{\pi}{2}\right) - E\left(k, \frac{\pi - \phi_c}{2}\right)\right\}\right]. \quad [9]$$

Fig. 1 (c) shows Δ in percentage as a function of D/a and $\bar{a}$.

The numerical calculations show that when $\theta_0 = 0^0$, $F_D > F_\infty$; when $\theta_0 = 180°$, $F_D < F_\infty$; and when $\theta_0 = 90°$, $F_D > F_\infty$ but the magnitude of the deviation becomes much smaller than when $\theta_0 = 0^0$. When $\bar{a} \equiv a\sqrt{(\varrho_2 - \varrho_3)g/\gamma_{23}}$ is large, the influence of the container wall is negligible for a relatively small D/a; but when $\bar{a}$ is small, the wall effect becomes significant even for a large D/a. Thus, when either the density difference across the interface is small or the interfacial tension is large, the wall effect should be taken into consideration. The influence of the container wall on the circular ring would be similar at least qualitatively to that for the cylinder, if we regard the ring wire as the cylinder. When the distance between the ring wire and the container wall is $2R$ and $R/a = 54$ (dimensions which are typical of those used in practice) the cylinder approximation yields $D/a = 108$; we thus expect that the wall effect for the ring will be generally small.

III. Approximate calculations of wall effect for a ring

When a circular ring is pulled through a finite liquid interface, liquid menisci with axial symmetry are formed inside and outside the ring, and they meet the ring surface at the coordinates (r_1, z_1) and (r_2, z_2), respectively, to form the contact line circles (fig. 2). To calculate the equilibrium force F acting on the ring we must know these coordinates, which can be obtained from the calculations of the equilibrium meniscus shapes. Since the exact meniscus shape require a lengthy numerical computation, we employ an approximate meniscus shapes available in the literature thus aiming for only an approximate estimate of the effect of D on γ_{23}.

The approximate location of the inner contact-line circle is, in terms of the dimensionless variables, given by (5)

$$\bar{z}_1 = 2\sin\left(\frac{\phi_1}{2}\right) + 2\left[1 - \cos^3\left(\frac{\phi_1}{2}\right)\right]/3\bar{R} \times \sin\left(\frac{\phi_1}{2}\right), \quad [10]$$

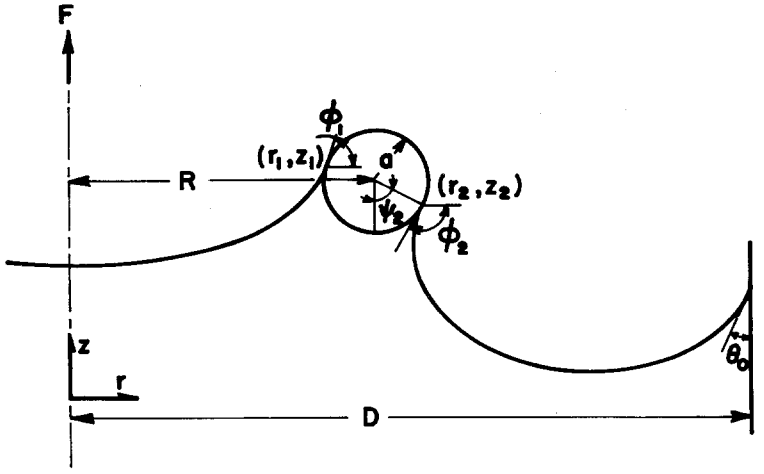

Fig. 2. A half section of a circular ring and the inner and outer menisci attached to it

and that of the outer contact line as (see Appendix)

$$\bar{z}_2 = 2\sin\left(\frac{\phi_2}{2}\right) + \frac{16\tan\left(\frac{\pi}{8}-\frac{\theta_0}{4}\right)}{\cos^2\left(\frac{\phi_2}{4}\right)} \times \exp\left[-\bar{D}+\bar{R} + 2\left\{\cos\left(\frac{\pi}{4}-\frac{\theta_0}{2}\right) + \cos\left(\frac{\phi_2}{2}\right) - 2\right\}\right] \quad [11]$$

where ϕ_1 and ϕ_2 are the angles between the axis of symmetry and the respective normal to the surface of the inner and outer meniscus at the contact line circle. These equations are valid when $\bar{R} \gg 1$, $\bar{D} \gg \bar{R}$ and $\bar{R} \gg \bar{a}$. In [10], $\bar{r}_1 = \bar{R} - \bar{a}\sin\phi_1$ has been replaced with $\bar{R}$ because $\bar{R} \gg \bar{a}$.

In actual use of the ring method the inner and outer menisci must make a zero angle of contact with the ring surface, in which event (fig. 2 and [3]–2)

$$[(\bar{z}_i - \bar{a}\cos\phi_i)(-1)^i]_2^1 = 0\,, \quad [12]$$

where

$$[\quad]_2^1 \equiv [\quad]_{i=1} + [\quad]_{i=2}\,.$$

The equilibrium force F acting on the ring is given ([8]–2 with $\bar{R} \gg \bar{a}$) in the dimensionless form

$$\bar{F} = 2\pi\bar{R}\left(\left[\left(1 - \frac{1}{2}\bar{a}^2\cos\phi_i + \bar{a}\bar{z}_i\right)\sin\phi_i + \frac{1}{2}\bar{a}^2\phi_i\right]_2^1 - \pi\bar{a}^2\right)\,. \quad [13]$$

As the ring is raised for given $\bar{R}$ and $\bar{a}$, a unique set of $(\phi_1, \bar{z}_1)$ and $(\phi_2, \bar{z}_2)$ determines $\bar{F}$; once ϕ_1 is determined, therefore, $\bar{F}$ is uniquely determined and we can regard $\bar{F}$ as a function of ϕ_1.

At the maximum force $\bar{F}_D$

$$\frac{d\bar{F}}{d\phi_1} = 0 = 2\pi\bar{R}\left[\left\{\bar{a}\left(\bar{a}\sin\phi_i + \frac{d\bar{z}_i}{d\phi_i}\right)\sin\phi_i + (1+\bar{a}\bar{z}_i)\cos\phi_i\right\}\frac{d\phi_i}{d\phi_1}\right]_2^1 = 2\pi\bar{R}\left[\bar{a}\sin\phi_i + \left\{(1+\bar{a}\bar{z}_i)\cos\phi_i\right\}\Big/\left(\frac{d\bar{z}_i}{d\phi_i} + \bar{a}\sin\phi_i\right)\right]_2^1, \quad [14]$$

where the derivatives $d\bar{z}_i/d\phi_i$ can be obtained from [10] and [11]. We eliminated $d\phi_2/d\phi_1$ in [14] by differentiating [12] with respect to ϕ_1 and inserting the resulting $d\phi_2/d\phi_1$ into [14]. The maximum force $\bar{F}_D$ can be calculated from [13], using the values $(\phi_1, \bar{z}_1)$ and $(\phi_2, \bar{z}_2)$ which satisfy [10], [11], [12] and [14].

When $\bar{D} \to \infty$, the values $(\phi_i, \bar{z}_i)$ at the contact line circles slightly change to $(\phi_i + \delta\phi_i, \bar{z}_i + \delta\bar{z}_i)$, and the force $\bar{F}$ on the ring to $\bar{F} + \delta\bar{F}$. We wish to know the change $\delta\bar{F}_D \equiv \bar{F}_\infty - \bar{F}_D$ as a function of $\bar{R}$, $\bar{a}$, $\bar{D}$ and θ_0. We can calculate the change in [11] as

$$\delta\bar{z}_2 = \cos\left(\frac{\phi_2}{2}\right)\delta\phi_2 - \frac{16\tan\left(\frac{\pi}{8}-\frac{\theta_0}{4}\right)}{\cos^2\left(\frac{\phi_2}{4}\right)} \times \exp\left[-\bar{D}+\bar{R}+2\left\{\cos\left(\frac{\pi}{4}-\frac{\theta_0}{2}\right) + \cos\left(\frac{\phi_2}{2}\right) - 2\right\}\right] + \mathcal{O}[(\delta\phi_2)^2]\,, \quad [15]$$

and the corresponding changes in [10], [12] and [13] are, respectively

$$\delta\bar{z}_1 = \left[\cos\left(\frac{\phi_1}{2}\right) + \cos^2\left(\frac{\phi_1}{2}\right)/\bar{R} - \cos\left(\frac{\phi_1}{2}\right)\left\{1 - \cos^3\left(\frac{\phi_1}{2}\right)\right\}\Big/\left\{3\bar{R}\sin^2\left(\frac{\phi_1}{2}\right)\right\}\right]\delta\phi_1\,, \quad [16]$$

$$[(\delta\bar{z}_i + \bar{a}\sin\phi_i\cdot\delta\phi_i)(-1)^i]_2^1 = 0\,, \quad [17]$$

$$\delta\bar{F} = 2\pi\bar{R}\left[\{\bar{a}^2\sin^2\phi_i + (1+\bar{a}\bar{z}_i)\cos\phi_i\}\,\delta\phi_i + \bar{a}\sin\phi_i\cdot\delta\bar{z}_i\right]_2^1\,. \quad [18]$$

We can eliminate $\delta\bar{z}_i$ and $\delta\phi_i$ from [15] to [18], and at the maximum force, we get after algebraic manipulation utilizing [14],

$$\delta\bar{F}_D = 32\pi\bar{R}\tan\left(\frac{\pi}{8}-\frac{\theta_0}{4}\right)\frac{\cos\phi_2}{\cos\left(\frac{\phi_2}{2}\right)\cos^2\left(\frac{\phi_2}{4}\right)} \times \exp\left[-\bar{D}+\bar{R}+2\left\{\cos\left(\frac{\pi}{4}-\frac{\theta_0}{2}\right)+\cos\left(\frac{\phi_2}{2}\right)-2\right\}\right]. \quad [19]$$

The maximum force corrected for D will therefore be $F_\infty = F_D + \delta F_D$, and the surface tension can be calculated as

$$\gamma_\infty = \gamma_D(1-\Delta), \quad [20a]$$

where

$$\Delta \equiv 16 f \tan\left(\frac{\pi}{8}-\frac{\theta_0}{4}\right) \times \frac{\cos\psi_2}{\sin\left(\frac{\psi_2}{2}\right)\left[1+\sin\left(\frac{\psi_2}{2}\right)\right]} \times \exp\left[-\sqrt{\frac{(\varrho_2-\varrho_3)g}{\gamma_D}}\,R\,(D/R-1)+2\left\{\sin\left(\frac{\psi_2}{2}\right)+\cos\left(\frac{\pi}{4}-\frac{\theta_0}{2}\right)-2\right\}\right], \quad [20b]$$

and γ_D is the tension without the correction for D; f is the Harkins-Jordan correction factor (1); and $\psi_2 = 180° - \phi_2$ is the location of the outer contact line circle on the ring surface, which is available from fig. 6(b) of ref. (2).

Fig. 3 shows Δ as a function of D/R and $\bar{R}$ when $\theta_0 = 0°$ and $R/a = 54$, the value used in the experiments described later.

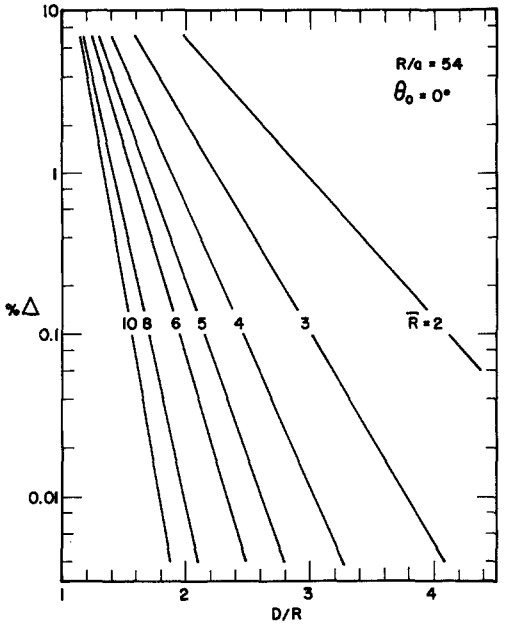

Fig. 3. The interfacial tension deviation Δ in percentage as a function of D/R and $\bar{R}$ when $R/a = 54$ and $\theta_0 = 0°$

IV. Experiments

The surface tension of water in air was measured by the ring method in two pyrex cells of different size. The cells, one 31 mm ID and 35 mm OD, and another 55 mm ID and 59 mm OD, were ground flat at the top with sharp inner and outer edges. The top plane was maintained horizontal to within 20′. The cells had a branching opening through which more water could be supplied to the cell. A platinum-iridium ring of $R = 0.9581$ cm and $R/a = 53.93$ was used; these dimensions are typical of those used in practice. The force exerted on the ring was measured with a Cahn RG microelectrobalance connected to a chart recorder, providing a resolution of 0.1 mg. The scheme of the experimental arrangement is shown in fig. 4. The cell was put in an enclosure for protection from the environment and for temperature control at 26.5 ± 0.1 °C; a thin wire attached to the weighing arm of the balance, above the cell enclosure, passed through a

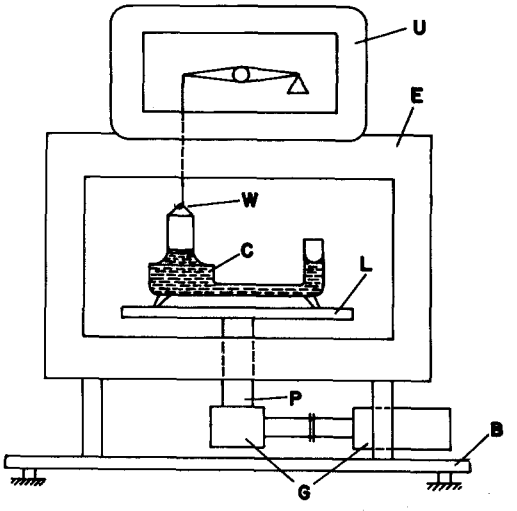

Fig. 4. Schematic of experimental arrangement. E – insulated enclosure with window; U – weighing unit of microelectrobalance; W – thin wire and duNouy ring; C – cell with branching opening; L – platform; P – piston; G – gears and motor; B – base with levelling legs

small hole on top of the enclosure, and was attached to the duNouy ring. The cell enclosure was mounted on a platform which could be moved vertically at constant low speeds by geared connections driven by a DC motor (Bodine).

Prior to use, the cell was washed with 2% Liquinox solution; rinsed with flowing tap water for an hour; immersed in an aqueous mixture of 2% hydrofluoric and 50% nitric acids; rinsed 15 to 20 times with distilled water; and used immediately without drying. The ring was rinsed in benzene; rinsed a few times in methyl-ethyl ketone; and flamed in a bunsen to dull red. Water, deionized, purified of organics and then distilled was used for the surface tension measurements.

In the first experiment, the cell was filled with water until it was on the brink of flowing over the outer edge of the cell. By raising the platform, the ring was immersed a few mm under the water surface. The movement of the platform was then reversed and it was lowered at a constant speed of about 0.5 mm/min., until the force exerted on the ring went through a maximum and started decreasing. The platform movement was again reversed to confirm that the force-displacement record was reproducible. We took the reproducibility obtained as an indication that the contact angle of the water with the ring surface was zero and thus exhibited no hysteresis, and that the platform movement was sufficiently slow enough to exclude any dynamic effects. The next experiment was identical to the previous one except that water was filled up to the inner edge of the cell, and then removed until the meniscus attached to the edge was about to detach and slide down the inner wall of the cell. In this way we created $\theta_0 = 180°$ at the wall for the first experiment and $\theta_0 = 0°$ for the second.

The results of experiments are summarized in table 1. The surface tension values have been calculated with the aid of our tables (2).

V. Discussion

The approximate theoretical analysis shows that the important parameters to be considered are the radius ratio D/R, the dimensionless ring radius $\bar{R}$, and the wall contact angle θ_0.

Table 1. Summary of experimental results

D (cm)	D/R	θ_0	γ_D (dyne/cm)	Calculated Δ (%)	Measured Δ (%)
2.95	3.079	180°	72.02	−0.023	−0.028
			71.98	−0.023	−0.083
2.75	2.870	0°	72.12	+0.049	+0.111
			72.13	+0.049	+0.125
1.75	1.827	180°	71.42	−1.95	−0.861

$R/a = 53.93$, $R = 0.9581$ cm, $\bar{R} = 3.539$, $\gamma_{23} = 72.04$ dyne/cm.

When the liquid interface was concave [viewed from the side toward which the ring is pulled ($\theta_0 < 90°$)], we obtained a high γ_D; when the interface was convex ($\theta_0 > 90°$), γ_D was too low. If the interface does not assume a constant angle of contact with the container wall, but sticks to the top edge of the container, the deviation from the true tension depends on whether the interface is convex or concave at the maximum force. Therefore, even if the interface is initially maintained flat at the top of the container, the interface becomes concave (viewed from above) at the maximum force because the volume displaced by the ring is filled in by the liquid, and we should get a higher tension value.

The experimental results of table 1 indicate that the approximate theory of Section III tends to overestimate the effect of the finite size of container for small D/R. This discrepancy may have resulted from adopting the approximate meniscus profiles [10] and [11], which assume $\bar{R} \gg 1$ and $D/R \gg 1$, and a more comprehensive study with the accurate profiles may be warranted. The approximation nevertheless provides an order of magnitude of the errors. As pointed out earlier (2), the deviation depends critically on the dimensionless ring radius $\bar{R} \equiv R\sqrt{(\varrho_2 - \varrho_3)g/\gamma_{23}}$. We see from fig. 3 ($R/a = 54$ and $\theta_0 = 0°$) that for $D/R = 3$, the error due to wall effect is less than 1% if $\bar{R} > 2$. When $D/R < 2.5$ and $\bar{R} < 2$, even though our approximate theory is then no more valid in this range, we may expect an error of 2% or more, and such a choice of D/R should be avoided. This may be done using a container of larger D rather than a ring of smaller R, because reducing $\bar{R}$ is not desirable. On the other hand, *Harkins* and *Jordan* (1) pointed out that with a small D/R (~ 2) it was not possible to measure the tension at all because the ring tended to cling to the side of the container. We may conclude that when $\bar{R} > 2$ and $D/R > 3$, we can expect a negligible wall effect, or it may result in the error in the same order of magnitude due to other reasons (2).

VI. Appendix

To calculate approximately the outer meniscus shape, we first assume that the azimuthal curvature of the meniscus is negligible com-

pared to the meridional curvature, because $\bar{R} \gg 1$. We then obtain from [3] and [4]

$$\bar{z}_2 = 2\left[\frac{1}{k^2} - \cos^2\left(\frac{\phi_2}{2}\right)\right]^{\frac{1}{2}}, \qquad [A1]$$

$$\bar{D} - \bar{R} = \left(\frac{2}{k} - k\right)\left[2F\left(k, \frac{\pi}{2}\right) - F\left(k, \frac{\pi - \phi_2}{2}\right) - F\left(k, \frac{\pi}{4} + \frac{\theta_0}{2}\right)\right] - \frac{2}{k}\left[2E\left(k, \frac{\pi}{2}\right) - E\left(k, \frac{\pi - \phi_2}{2}\right) - E\left(k, \frac{\pi}{4} + \frac{\theta_0}{2}\right)\right], \qquad [A2]$$

where $\bar{r}_2 = \bar{R} + \bar{a}\sin\phi_2$ has been replaced with $\bar{R}$ because $\bar{R} \gg \bar{a}$.

If we further assume that $\bar{D} \gg \bar{R}$, k becomes near unity, and we may approximate the above equations in terms of $(1-k) \ll 1$:

$$\bar{z}_2 = 2\sin\left(\frac{\phi_2}{2}\right) + \frac{2(1-k)}{\sin\left(\frac{\phi_2}{2}\right)} + \mathcal{O}((1-k)^2), \qquad [A3]$$

$$\bar{D} - \bar{R} = \ln\left(\frac{16}{1-k}\right) + \ln\frac{\tan\left(\frac{\pi}{8} - \frac{\theta_0}{4}\right)}{\cot\left(\frac{\phi_2}{4}\right)} + 2\left\{\cos\left(\frac{\phi_2}{2}\right) + \cos\left(\frac{\pi}{4} - \frac{\theta_0}{2}\right) - 2\right\} + \mathcal{O}(1-k). \qquad [A4]$$

Eliminating $(1-k)$ from [A3] and [A4], we get [11].

Acknowledgement

The authors are grateful to *A. Mar* for the experimental work. This research was supported by the Defense Research Board Grant No 9530-47.

Summary

As a supplement to our theoretical calculations for the ring method of measuring surface and interfacial tensions of liquids, the effect of the finite size of the liquid container on the measurement has been studied employing (i) an exact analysis for the case of an infinite straight cylinder midway between two parallel walls and (ii) an approximate analysis for a ring in a circular container. The parameters which can cause errors are identified, and their magnitude is estimated and compared with the experimental results for surface tension of water in air. It is shown that conditions can be readily adjusted to produce negligible errors.

References

1) *Harkins, W. D., H. F. Jordan*, J. Amer. Chem. Soc. **52**, 1751 (1930).

2) *Huh, C., S. G. Mason*, Colloid & Polymer Sci. **253**, 566 (1975).

3) *Princen, H. M., S. G. Mason*, J. Colloid Interf. Sci. **20**, 246 (1965).

4) *Princen, H. M.*, Surface and Colloid Science, Vol. 2 (New York 1969).

5) *Blaisdell, B. E.*, J. Math. Phys. **19**, 228 (1940).

Author's address:

S. G. Mason
McGill University,
Department of Chemistry,
P. O. Box 6070, Station 'A',
Montreal, Quebec H3C 3G1 (Canada)